

MECHANICAL ENGINEERING

Effect of electrode material on electrical discharge machining of tool steel surface



Mona A. Younis ^{a,*}, Mohamed S. Abbas ^b, Mostafa A. Gouda ^c,
Fouad H. Mahmoud ^d, Sayed A. Abd Allah ^d

^a Mechanical Engineering Department, Higher Technological Institute, Tenth of Ramadan City, Egypt

^b Modern University for Technology and Information, Egypt

^c Mechanical Engineering Department, British University in Egypt, Egypt

^d Mechanical Engineering Department, Shoubra Faculty of Engineering, Banha University, Egypt

Received 10 November 2014; revised 14 February 2015; accepted 18 February 2015

Available online 6 May 2015

KEYWORDS

EDM;
DIN 1.2080;
DIN 1.2379;
Electrode;
POCO graphite;
Dura graphite

Abstract In this study the effect of electrode material was studied to avoid resulting residual stresses, the surface roughness and cracks resulted during Electrical Discharge Machining (EDM). Two types of EDM electrode materials were chosen, Dura graphite 11 and POCO graphite EDMC-3. Two grades of tool steels are chosen as test materials, DIN 1.2080 and DIN 1.2379. Different machining methods were chosen “rough, medium, and soft”, it was found that the Dura graphite 11 exhibits more surface cracks upon DIN 1.2379 less micro-cracks appeared on the surface than on DIN 1.2080 while the higher surface roughness appeared in DIN 1.2080 using Dura Graphite 11 electrode, also Residual stresses were studied upon the surface and it was found that POCO Graphite EDMC-3 electrode results higher residual stresses compared with Dura Graphite 11 electrode. Also Soft EDM machining exhibits higher residual stresses as a result of higher pulse on duration time.

© 2015 Faculty of Engineering, Ain Shams University. Production and hosting by Elsevier B.V. This is an open access article under the CC BY-NC-ND license (<http://creativecommons.org/licenses/by-nc-nd/4.0/>).

1. Introduction

1.1. EDM principle

Electrical Discharge Machining (EDM) is one of the most successful and extensively recognized processes for the production

of tiny apertures with high accuracy and complicated profiles [1]. This method is commonly used in manufacturing of molds and dies in hardened steels. These hard and brittle materials manufactured by conventional machining operations produce extreme tool wear and expense. The mechanical properties of tool steels have been studied extensively for many years [2,3]. During the EDM machining, the workpiece and the tool are separated by a tiny gap, and immersed in dielectric fluid. The discharge energy generates excessive temperatures on the surface of the workpiece during the spark. The specimen is exposed to a temperature increase up to 30,000 °C melting a tiny part of the workpiece and vaporizing it. The upper surface of the workpiece consequently solidifies quickly (Fig. 1). At the

* Corresponding author. Tel.: +20 1224519266.

E-mail address: mona.younis@hti.edu.eg (M.A. Younis).

Peer review under responsibility of Ain Shams University.



Production and hosting by Elsevier

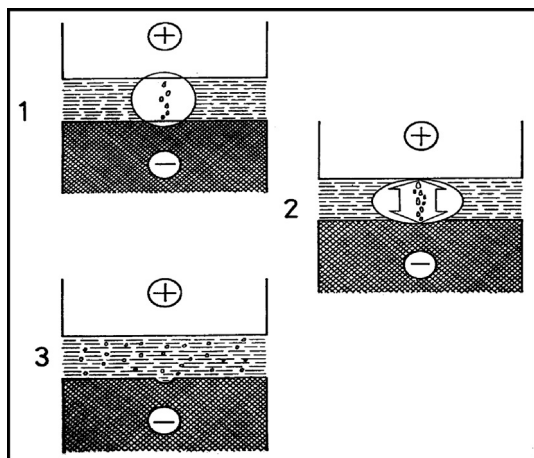


Figure 1 One machining cycle of EDM process.

point at which the spark occurs, the current is converted into heat and the workpiece is strongly heated. If the current is interrupted, the discharge channel explosively evaporates, carrying away melted material from the workpiece. This leaves a small crater. Should discharge resume the crater will grow, removing more and more materials. Since there is no contact between cutting tool and work-piece and no physical force applied, the shape being cut will exactly match the shape of the electrode [4].

Previous research has shown that the quality of the machined surface is determined primarily by the pulse current and the pulse-on duration time [5–15] but few literatures studied the effect of electrode material [16–23]. Accordingly, the current study is based upon these two parameters, and specifies pulse currents of 15, 30 and 50 A with pulse-on times of 20, 100, 180 μs . Using two grades of electrode materials (Dura Graphite 11 and Poco Graphite EDMC-3) as test electrodes. After completion of the EDM machining process, the surface integrity of the sample material is examined using Scanning electron Microscopy (SEM) then measuring residual stresses using X-ray Diffraction (XRD). The machining conditions are presented in Fig. 2.

2. Experimental work

2.1. Test electrodes

Two grades of electrode materials have been chosen; Dura Graphite 11 is widely used in the Egyptian market because

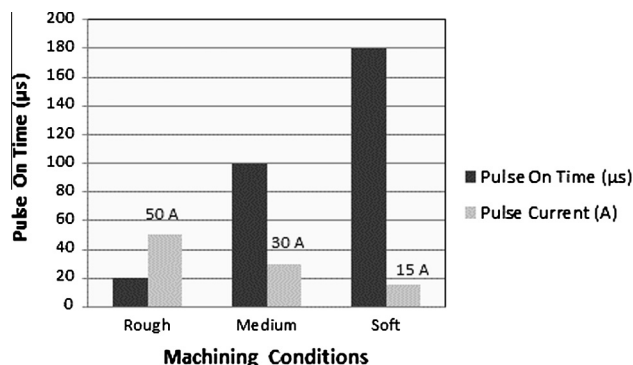


Figure 2 Machining conditions.

they can be easily and cheaply prepared. Graphite has a very high melting point. Truly, graphite does not melt at all, but transform directly from solid to gas at a temperature thousands of degrees (3200 $^{\circ}\text{C}$) higher than the melting point of Copper. This temperature resistance makes graphite an ideal electrode material [24]. Also Graphite electrodes can offer great levels of electrical conductivity. POCO's EDMC-3 is widely used in the Egyptian market, it is a high quality graphite penetrated with copper, suggested where wear, speed, and surface finish are valuable. Matchless for brittle electrodes, many EDM users select this grade to balance for operator immaturity or where bad flushing conditions exist. Tables 1 and 2 show the Physical characteristics of Dura Graphite 11 graphite and POCO graphite EDMC-3 respectively.

2.2. Test materials

Two grades of tool steels have been chosen; DIN 1.2080 is a high carbon, high chromium alloy tool steel with excellent resistance to wear and abrasion high-performance blanking and punching dies for sheet thickness up to 1.5 mm; threads rolling dies, plastic molds. DIN 1.2379 is a high carbon, high chromium, molybdenum, vanadium tool steel which offers good wear resistance, high-performance blanking and punching dies for sheet thickness up to 3 mm; thread rolling dies, plastic molds. Also DIN 1.2080 and DIN 1.2379 tool steel materials are widely used in the Egyptian market Tables 3 and 4 show the typical analysis of DIN 1.2080 and DIN1.2379 respectively.

2.3. Experimental procedures

To prepare the EDM specimens, the base specimens were machined by EDM to remove the unnecessary material at various machining conditions “rough, medium and soft” according to pulse current (A) and pulse-on duration time (μs) presented in Fig. 2, then scanning the specimen with scanning electron microscope (SEM) to study the effect of electrode material upon the test material to avoid the surface roughness and cracks, then residual stress measurement using x-ray diffraction.

2.4. X-ray diffraction calculations

The average size (L) of the DIN 1.2080 and DIN 1.2379 nanocrystallites and the lattice strain (ζ) of the film were calculated using Eq. (1)

$$\beta \cos \theta = 4\zeta \sin \theta + \frac{k\lambda}{L} \quad (1)$$

where λ is X-ray wavelength of the Cu $K\alpha_1$ radiation, θ is the Bragg angle, K is the shape factor which is almost unity, and β

Table 1 Physical characteristics of Dura graphite 11 graphite.

Average particle size (μm)	10
Compressive strength (MPa)	83.4
Electrical resistivity ($\mu\Omega \text{ m}$)	11
Melting point ($^{\circ}\text{C}$)	3000
Thermal conductivity (W/m K)	120

Table 2 Physical characteristics of POCO graphite EDMC-3.

Average particle size (μm)	< 5
Compressive strength (MPa)	206
Electrical resistivity ($\mu\Omega\text{ m}$)	3.2
Melting point ($^{\circ}\text{C}$)	1100
Thermal conductivity (W/m K)	135

is the full-width at half-maximum (FWHM) of the XRD peak appearing at the diffraction angle θ .

The β parameter in the above equation must be corrected with the instrumental width through using of the geometric mean,

$$\beta = \sqrt{(\beta_{exp} - \beta_{inst}) \sqrt{(\beta_{exp}^2 - \beta_{inst}^2)}} \quad (2)$$

where β_{exp} and β_{inst} parameters are the experimental and the instrumental linear widths in radians, respectively. The value of β_{inst} was determined to be 2.58×10^{-3} rad. by using a standard silicon powder. Thus from Fig. 3, it is clear that when $\beta \cos \theta$ is plotted against $\sin \theta$ a straight line with slope 4ζ and intercept $K\lambda/L$ is obtained. From the slope of this straight line the strain of the lattice can be calculated [25].

3. Results and discussion

After the EDM process the test materials were examined using scanning electron microscope to observe the surface cracks, roughness, and then X-ray diffraction to examine the residual stresses generated after the three machining conditions using the test electrodes.

3.1. SEM observation

The characteristic morphology of a surface which has experienced EDM machining, is due to the extensive amount of heat generated by the discharge current, which causes melting and evaporation of the material, then fast cooling. It is seen after rough machining, the surface is rougher and the machined surface contains lots of globules, melted drops and craters, and reduces with medium and soft machining. This is due to very high temperature gradient produced due to the thermal energy in the work-piece erosion happens from the surface and the debris particles remain on the work-piece surface. Surface morphology observations using Dura Graphite 11 and POCO graphite EDMC-3 electrodes have been presented as follows in Figs. 4–9.

Fig. 10 shows the surface roughness observations. It was found that it is approximately the same for DIN 1.2080 and DIN 1.2379, in both electrodes, the surface roughness increase as the pulse current increase. This is because at rough machining whenever peak current increases more intensely discharges which effect on the surfaces, more quantity of molten and

floating metal are suspended in the gap between tool and work-pieces resulting increase the surface roughness. Also it is clear that Dura graphite exhibits higher surface roughness upon DIN 1.2080 surface during all machining conditions and this is due to Dura graphite 11 composition, it is a compressed graphite powder which erodes easily during machining, and also due to the higher carbon content in DIN 1.2080 “Table 3” which solidifies upon the surface during solidification and not flushed away.

3.1.1. Cracks observations

Observations of the EDMed surface show that the surface cracks are often micro-cracks in both test material and electrodes. The scanning electron microscope shows that cracks occur in the white layer surface; as shown in Figs. 11–18. It is found that microcracks decrease as pulse current decrease. This effect can be explained that high energy causes a sharp thermal gradient below the melting zone. The machined layer generated by the EDM process produces a destructive effect decreasing the service strength and life of the parent material. This damaged layer should be removed before being to use. It is therefore recommended that the EDM specimen should be polished down to at least the maximum depth of the micro-cracks in order to improve its service life.

3.2. Residual stresses observations

A new mathematical model was designed using DESIGN EXPERT software to analyze the results, full factorial design was selected and analysis of variance (ANOVA) was utilized to evaluate the results. Table 5 shows obtained residual stresses of DIN1.2080 and DIN 1.2379 specimens using XRD analysis. Table 6 shows the selected factors operated for this study within working levels. Three factors and three levels were used in this experiment. There are 12 running processes were performed from the equation of full factorial design. The equation of full factorial design is stated in equation

$$\text{Full factorial equation} = 2^k \quad (3)$$

where k denotes as the number of factors, i.e., machining conditions, test material, and electrode material, being examined in this experiment and three levels of experiment are employed, i.e., low (–1), med. (0), and high (+1).

The analysis of ANOVA is utilized to specify the EDM machining characteristics mathematical model using DESIGN EXPERT software version 9. Table 6 shows the design model used in ANOVA analysis.

Based on ANOVA analysis of Residual Stress in Table 7, it can be seen that the model is significant with probability, Prob > F value between 0.0001 and 0.0478 less than 0.05. It shows that Factor A electrode material, and Factor C machining conditions are significant (see Table 8).

Fig. 19 displays the normal probability plot of residuals are presented on a straight line; this means that the errors are

Table 3 DIN 1.2080 typical analysis.

C	Si	Cr	Mn
2.10%	0.30%	12.50%	0.30%

Table 4 DIN 1.2379 typical analyses.

C	Si	Cr	Mo	V
1.50%	0.30%	12.0%	0.80%	0.80%

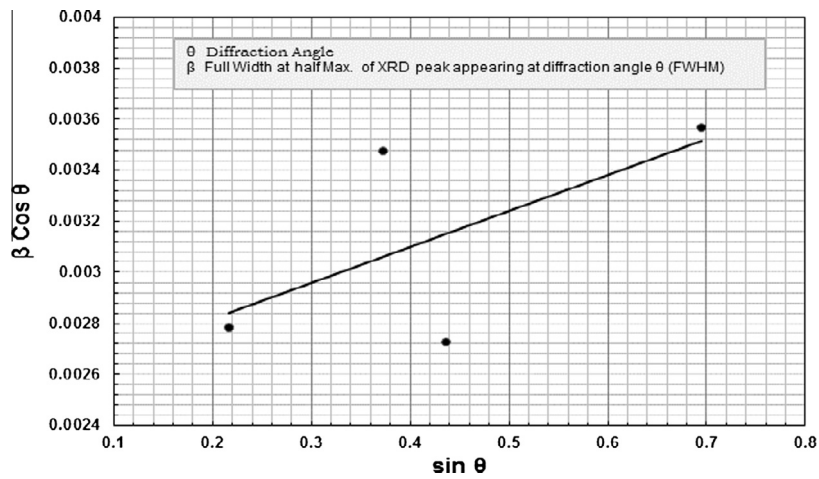


Figure 3 Plot of $\beta \cos \theta$ vs. $\sin \theta$.

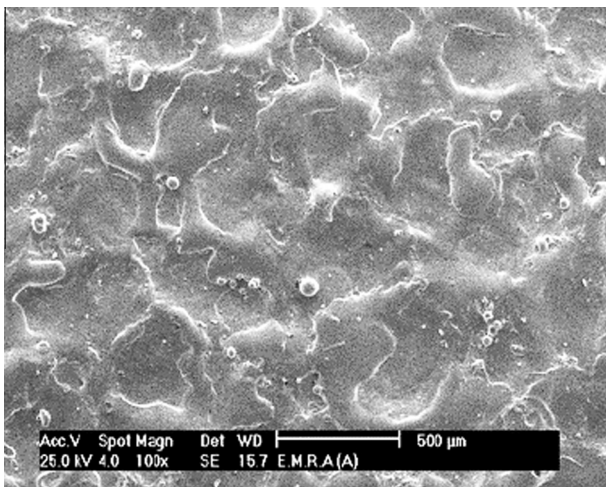


Figure 4 Dura graphite 11 rough machining DIN 1.2379.

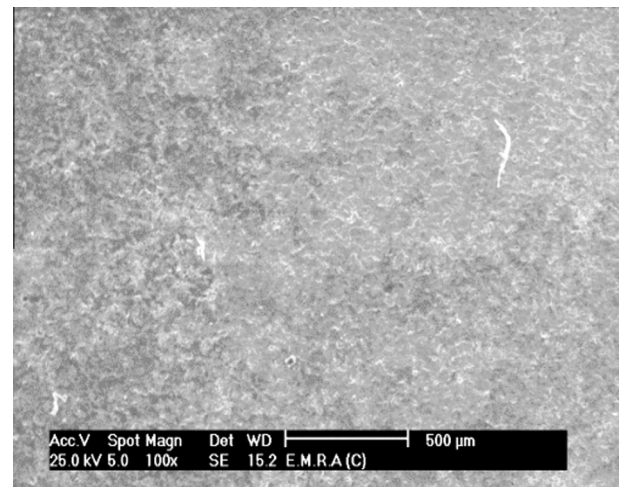


Figure 6 Dura graphite 11 soft machining DIN 1.2379.

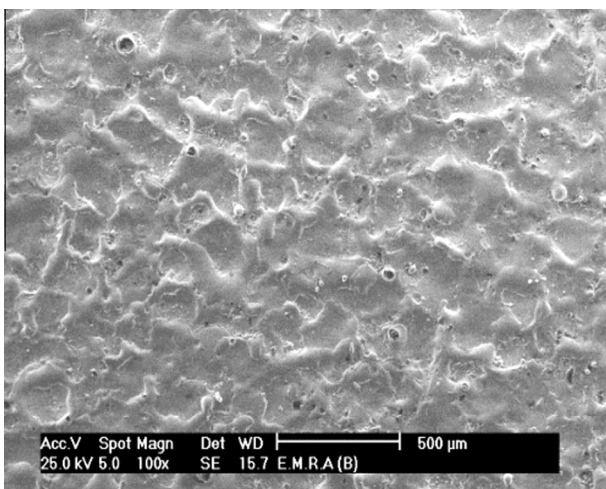


Figure 5 Dura graphite 11 medium machining DIN 1.2379.

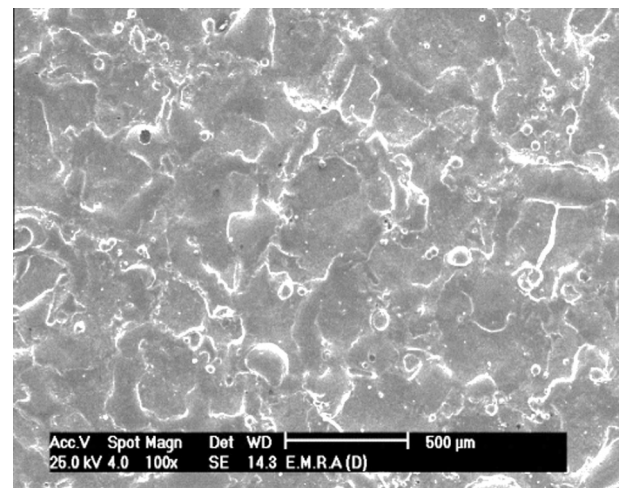


Figure 7 POCO graphite EDMC-3 rough machining DIN 1.2379.

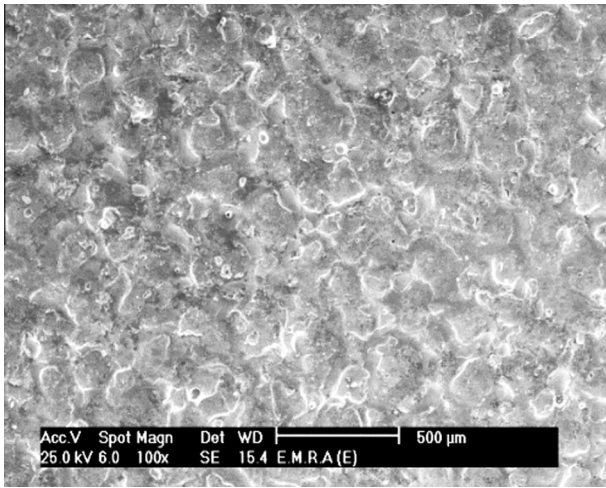


Figure 8 POCO graphite EDMC-3 medium machining DIN 1.2379.

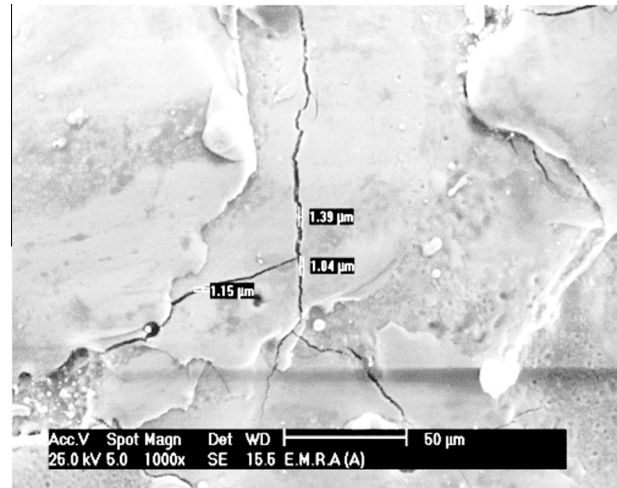


Figure 11 Surface cracks of DIN 1.2379 rough machining using Dura graphite 11 electrode.

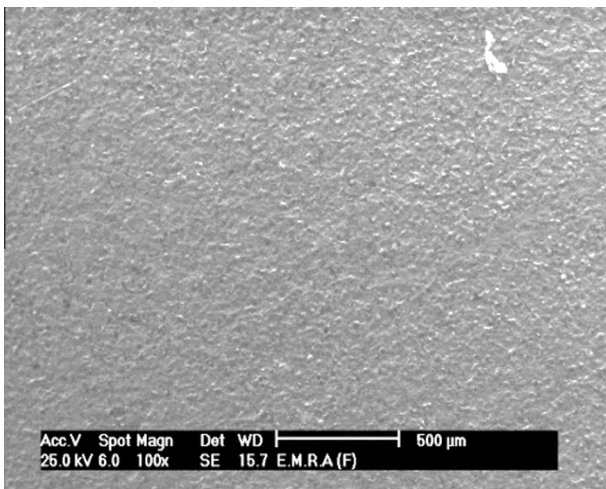


Figure 9 POCO graphite EDMC-3 soft machining DIN 1.2379.

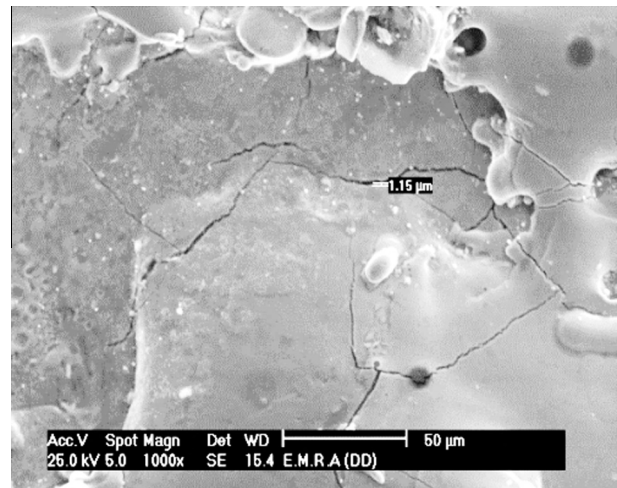


Figure 12 Surface cracks of DIN 1.2080 rough machining using POCO graphite EDMC-3 electrode.

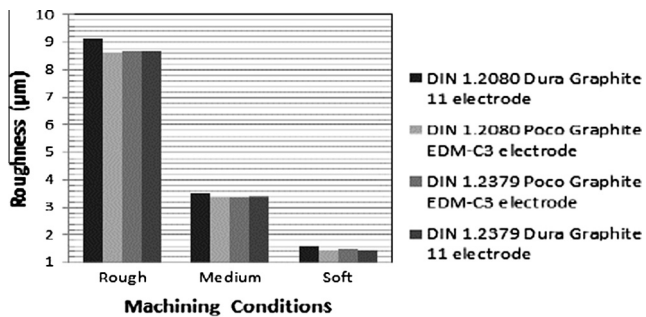


Figure 10 Surface roughness observations.

normally distributed. Further, each observed value is compared with the predicted value calculated from the model in Fig. 20. It can be seen that the regression model is fairly well fitted with the observed values.

The response ranges from 26.25 MPa to 1239 MPa and the ratio of maximum to minimum is 47.2. After eliminating the

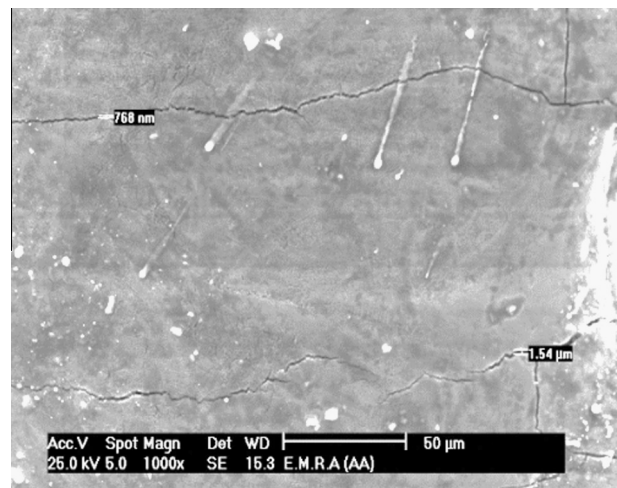


Figure 13 Surface cracks of DIN 1.2080 rough machining using Dura graphite 11 electrode.

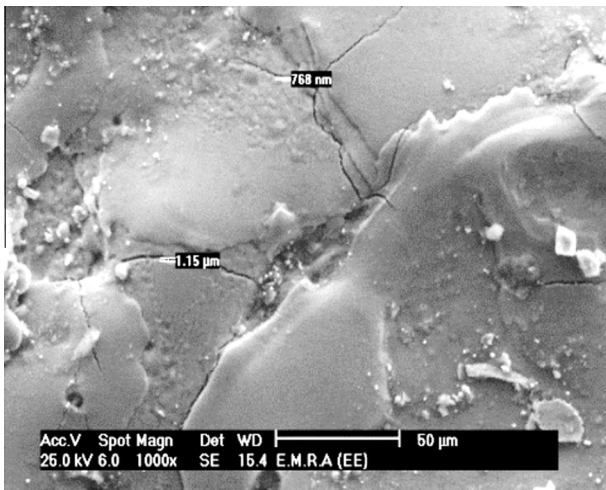


Figure 14 Surface cracks of DIN 1.2080 medium machining using POCO graphite EDMC-3 electrode.

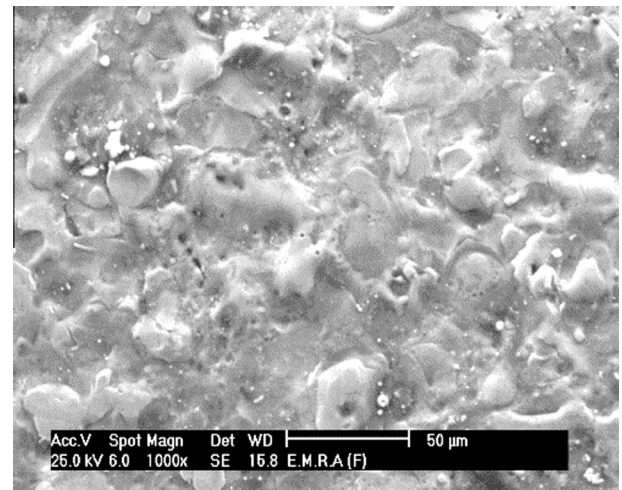


Figure 17 Surface cracks of DIN 1.2379 soft machining using POCO graphite EDMC-3 electrode.

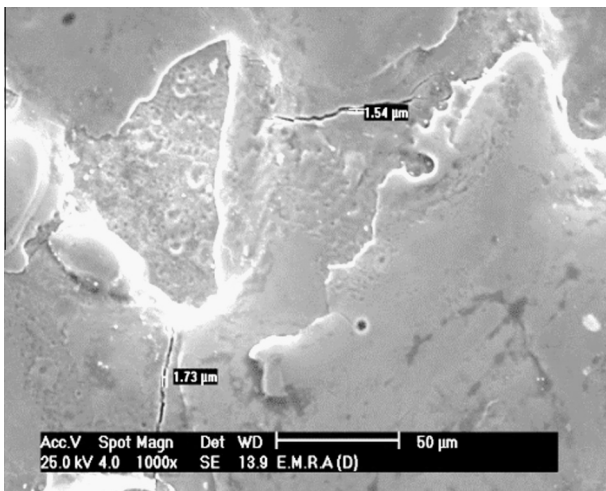


Figure 15 Surface cracks of DIN 1.2379 rough machining using POCO graphite EDMC-3 electrode.

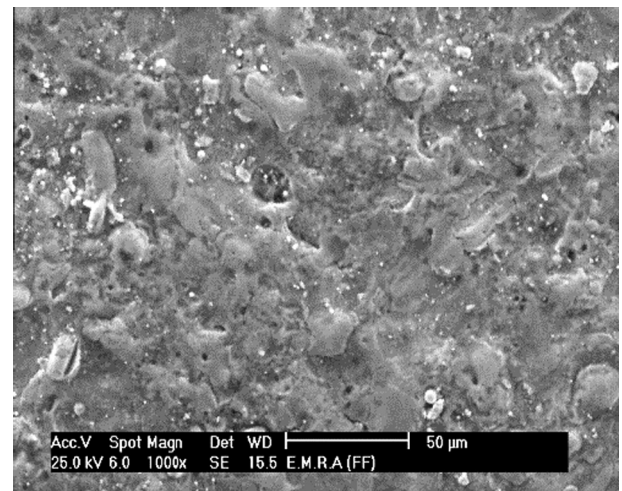


Figure 18 Surface cracks of DIN 1.2080 soft machining using POCO graphite EDMC-3.

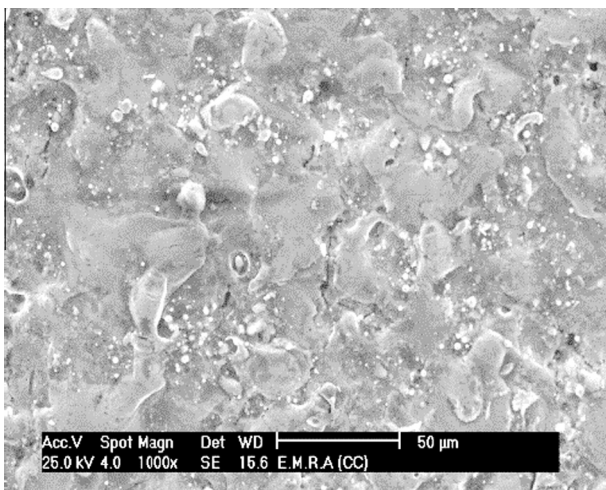


Figure 16 Surface cracks of DIN 1.2080 soft machining using Dura graphite 11 electrode.

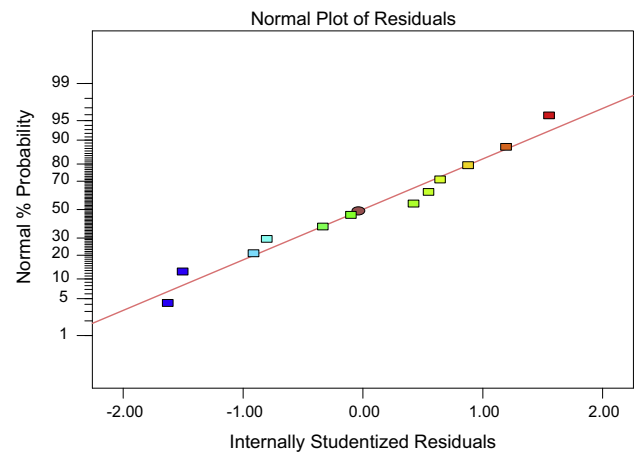


Figure 19 Displays the normal probability plot of residuals.

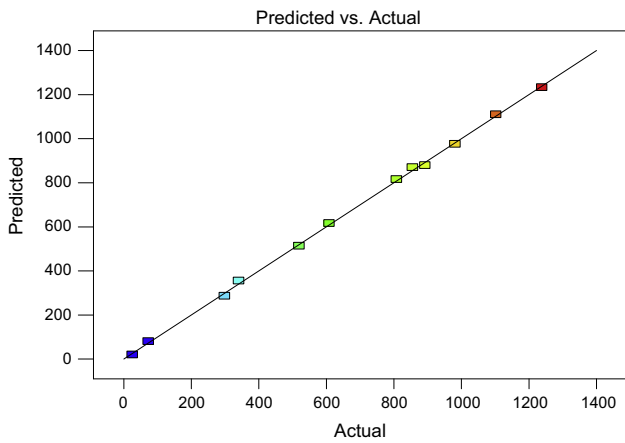


Figure 20 Predicted vs. Actual values of Residual stress.

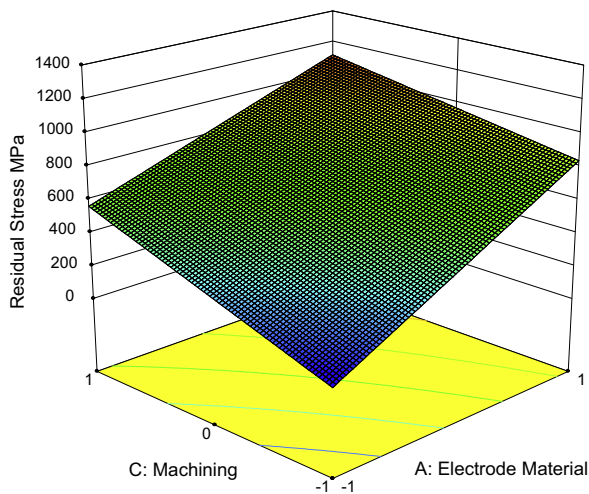


Figure 21 The estimated response 3D surface for Residual Stress in relation to the design parameters of Electrode Material and Machining.

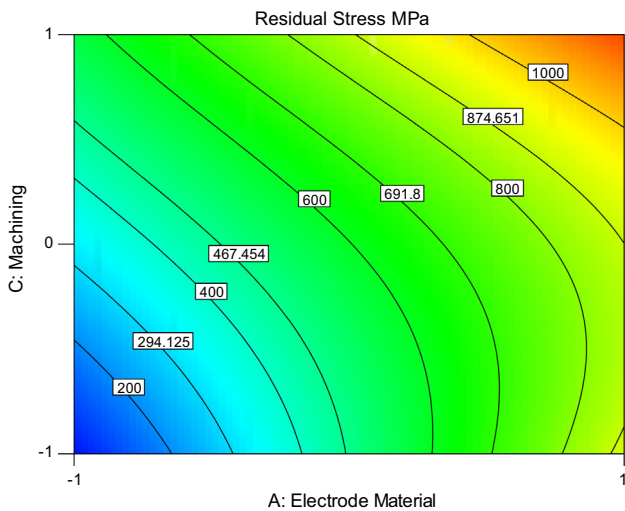


Figure 22 The estimated response Contour for Residual Stress in relation to the design parameters of Electrode Material and Machining.

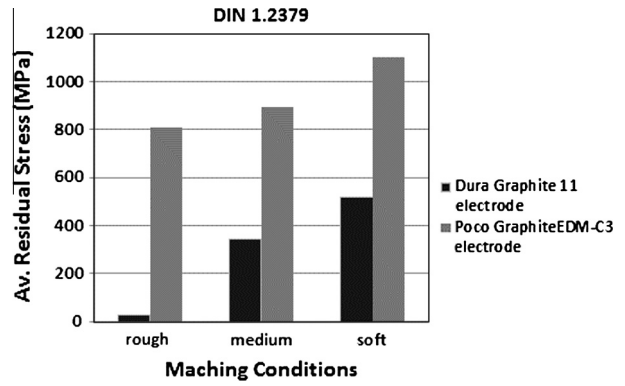


Figure 23 Average residual stresses for DIN 1.2379.

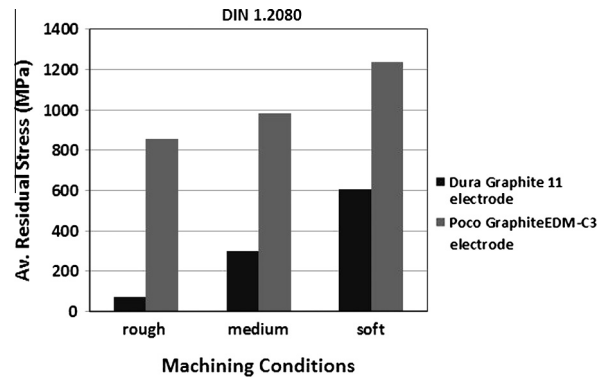


Figure 24 Average residual stresses for DIN 1.2080.

Table 5 Obtained stress of DIN1.2080 and DIN 1.2379 specimens.

Material	Av. Residual Stress (MPa)
DIN 1.2379 rough machined by Dura graphite 11	26.25
DIN 1.2080 rough machined by Dura graphite 11	73.5
DIN 1.2379 medium machined by Dura graphite 11	341.25
DIN 1.2080 medium machined by Dura graphite 11	299.25
DIN 1.2379 soft machined by Dura graphite 11	519.75
DIN 1.2080 soft machined by Dura graphite 11	609
DIN 1.2379 rough machined by POCO graphite EDM-C 3	808.5
DIN 1.2080 rough machined by POCO graphite EDM-C 3	981.75
DIN 1.2379 medium machined by POCO graphite EDM-C 3	892.5
DIN 1.2080 medium machined by POCO graphite EDM-C 3	855.75
DIN 1.2379 soft machined by POCO graphite EDM-C 3	1102.5
DIN 1.2080 soft machined by POCO graphite EDM-C 3	1239

Table 6 The selected parameters performed for this study with working levels.

Coded levels	1	0	-1
Electrode Material	POCO Graphite EDM-C3	-	Dura Graphite 11
Machining	Soft	Medium	Rough

Table 7 Design model used in ANOVA analysis.

Run	Factor 1 A: Electrode Material	Factor 2 B: Material	Factor 3 C: Machining	Response Residual Stress (MPa)
1	1	-1	0	892.5
2	-1	-1	0	341.25
3	1	1	-1	981.75
4	1	-1	-1	808.5
5	1	1	1	1239
6	1	-1	1	1102.5
7	-1	-1	-1	26.25
8	-1	-1	1	519.75
9	-1	1	-1	73.5
10	1	1	0	855.75
11	-1	1	0	299.25
12	-1	1	1	609

non-significant terms, the final response equation for residual stress is given as follows:

$$\text{Residual Stress} = 645.75 + 334.25 \times A + 197.53 \times C \tag{4}$$

where *A* is the Electrode Material and *C* is the Machining Conditions.

Equation in terms of all coded factors:

$$\begin{aligned} \text{Residual Stress} = & 597.19 + 276.94 \times A - 19.69 \times B \\ & + 197.53 \times C + 1.31 \times AB - 59.72 \\ & \times AC + 0.66 \times BC + 72.84 \times C^2 \\ & - 9.84 \times ABC + 85.97 \times AC^2 + 75.47 \\ & \times BC^2 + 20.34 \times ABC^2 \end{aligned} \tag{5}$$

Eqs. (4) and (5) are multiple regression model based on the data collected during the course of the experiment “Table 5”.

Figs. 21 and 22 show the estimated response in 3D surface and contour respectively for Residual Stresses in relation to the design parameters of Electrode Material and Machining. The Residual Stress tends to increase considerably with soft machining using Poco graphite electrode. It is clear from the figure that the lower residual Stress can be obtained using rough machining with Dura graphite electrode.

Residual Stresses Observations found that soft machining in both electrode and materials results higher residual stresses compared with medium and rough machining and this is due to higher pulse on duration time in soft machining, and POCO Graphite EDMC-3 electrode exhibited higher residual stresses compared with Dura Graphite 11 electrode. As a result that POCO graphite EDMC-3 composition which is high quality graphite infiltrated with copper as shown in Figs. 23 and 24.

4. Conclusions

1. It was found that Dura graphite exhibited higher surface roughness upon DIN 1.2080 surface during all machining conditions and this is due to its composition, it is a compressed graphite powder which erodes easily during machining, and also due to the higher carbon content in DIN 1.2080 which solidifies upon the surface during solidification and not flushed away.
2. Rough EDM machining exhibited more micro-cracks as a result of higher pulse current.

Table 8 ANOVA analysis of Residual Stress.

Response: Residual Stress						
ANOVA for response surface cubic model						
Analysis of variance table [Partial sum of squares – Type II]						
Source	Sum of squares	df	Mean square	F value	P-value Prob. > F	
Model	1,745,091	10	174509.0977	158.12	0.06182	Not significant
A-Electrode Material	306,778	1	306777.5156	277.967	0.03814	
B-Material	1550.39	1	1550.390625	1.40479	0.44616	
C-Machining	312,149	1	312148.7578	282.834	0.03781	
AB	2655.19	1	2655.1875	2.40583	0.36456	
AC	28530.6	1	28530.63281	25.8512	0.12363	
BC	3.44531	1	3.4453125	0.00312	0.96447	
C ²	14149.9	1	14149.89844	12.821	0.17338	
ABC	775.195	1	775.1953125	0.70239	0.55593	
AC ²	19708.3	1	19708.33594	17.8574	0.14793	
BC ²	15188.1	1	15188.08594	13.7617	0.16763	
Residual	1103.65	1	1103.648438			
Pure error	0	0				
Cor total	1,746,195	11				

3. Soft machining in both electrodes and materials exhibited higher residual stresses compared with medium and rough machining and this is due to higher pulse on duration time in soft machining.
4. POCO Graphite EDMC-3 electrode exhibited higher residual stresses compared with Dura Graphite 11 electrode. As a result that POCO graphite EDMC-3 composition which is a high quality graphite infiltrated with copper.
5. According to ANOVA used the most significant parameter affecting residual stresses occurred during EDM machining were the Electrode Material and Machining condition "rough, medium or soft".

References

- [1] Darji Y, Koradiya PL, Shah JR. Experiment investigation of EDM parameter MRR and TWR with multi wall carbon nano tubes. *Int J Mech Eng Technol (IJMET)* 2014;5(7):84–192.
- [2] Cullity BD. *Elements of X-ray diffraction*. 2nd ed. Addison Wesley; 1978, p. 470.
- [3] Hilley ME, editor. *Residual stress measurement by XRay diffraction*. SAE J784a. Warrendale, PA: Society of Automotive Engineers; 1971. p. 19.
- [4] Chen PW. Size effect on the surface roughness and surface crack of EDMed surface. Master thesis, Department of Mechanical Engineering, National Cheng Kung University, Tainan, Taiwan; 2003.
- [5] El-Hofy H. *Advanced machining processes, nontraditional and hybrid machining processes*. McGraw-Hill; 2005.
- [6] Kumar Sh. Experimental investigation of machining parameters for EDM using U-shaped electrode of AISI P20 tool steel. MThesis, National Institute of Technology Rourkela India; 2010.
- [7] Arikatla SP, Krishnaiah A, Mannan KT. Optimization of electric discharge machining response variables using design of experiments. *Int J Mech Prod Eng (IJMPE)* 2013;2(1).
- [8] Khundrakpam NS, Singh H, Kumar S, Brar GS. Investigation and modeling of silicon powder mixed EDM using response surface method. *Int J Curr Eng Technol* 2014.
- [9] Kuriachen B, Paul J, Mathew J. Modeling of wire electrical discharge machining parameters using titanium alloy (Ti–6Al–4V). *Int J Emerg Technol Adv Eng* 2012;2(4).
- [10] Anayet Md, Patwari U, Chowdhury NA, Arif MD, Chowdhury MdSI. Surface roughness optimization in EDM for circular copper electrode by RSM-Ga approach. *Int J Eng* 2012.
- [11] Lee HT, Ehbach WP, et al. Relationship between electrode size and surface cracking in the EDM machining process. *J Mater Sci* 2004;39(23):6981–6.
- [12] Shabgard MR, zavvar MS, Babil SN. Influence of input parameters on the characteristics of the EDM process. *J Mech Eng* 2011;689–96.
- [13] Lauwers B, Kruth JP, Liu W, Eeraerts W, Schacht B, Bleys P. Investigation of material removal mechanisms in EDM of composite ceramic materials. *J Mater Process Technol* 2004: 347–52.
- [14] Dasa MK, Kumarb K, Barmana TK, Sahoo P. Application of artificial bee colony algorithm for optimization of MRR and surface roughness in EDM of EN31 tool steel. *Proc Mater Sci* 2014;741–51.
- [15] Vikas, Roy AK, Kumar K. Effect and optimization of various machine process parameters on the surface roughness in EDM for an EN41 material using Grey Taguchi. *Proc Mater Sci* 2014: 383–90.
- [16] Moudood* MA, Sabur A, Lutfi A, Ali MY, Jaafar IH. Investigation of the machinability of non-conductive ZrO₂ with different tool electrodes in EDM. *Int J Autom Mech Eng* 2014;10:1866–76.
- [17] Janmanee P, Muttamara A. Performance of difference electrode materials in electrical discharge machining of tungsten carbide. *Energy Res J* 2010:87–90.
- [18] Muthuramalingam T, Mohan B. Influence of tool electrode properties on machinability in spark erosion machining. *Mater Manuf Process* 2013;28(8):939–43.
- [19] Muthuramalingam T, Mohan B, Jothilingam A. Effect of tool electrode resolidification on surface hardness in electrical discharge machining. *Mater Manuf Process* 2014;29(11–12):1374–80.
- [20] Amorim FL, Weingaertner WL. The behavior of graphite and copper electrodes on the finish die-sinking electrical discharge machining (Edm) of Aisi P20 tool steel. *J Braz Soc Mech Sci Eng* 2007;Xxix(4/367).
- [21] Kumar N, Kumar L, Tewatia H, Yadav R. Comparative study for Mrr on die-sinking EDM using electrode of copper & graphite. *Int J Adv Technol Eng Res (IJATER)* 2012;2(2):170–4, ISSN 2250-3536.
- [22] Janmanee P, Muttamara A. Performance of difference electrode materials in electrical discharge machining of tungsten carbide. *Energy Res J* 2010;1(2):87–90, ISSN 1949-015.
- [23] Jha B, Ram K, Rao M. An overview of technology and research in electrode design and manufacturing in sinking electrical discharge machining. *J Eng Sci Technol Rev* 2011;4(2):118–30.
- [24] Kern Roger. Sinkler electrode material selection. *EDM Today*; July/August 2008 Issue.
- [25] Lifshin E. *X-ray characterization of materials*. New York: Wiley-VCH; 1999.



Mona Ahmed Sayed Younis completed her bachelor's in Mechanical Engineering from Higher Technological Institute in 2003. She has master's and doctoral degrees in Science of Mechanical Engineering from Shoubra Faculty of Engineering, Banha University completed in 2009 and 2015 respectively. She has teaching experience as Assistant in Higher Technological Institute, tenth of Ramadan city, Egypt, since 2003.



Mohamed S. Abbas is a Professor in Mechanical Engineering Department, Shoubra Faculty of Engineering, Banha University, Egypt also he is the Vice President of Modern University for Technology and Information, Egypt.



Mostafa A. Gouda is an active member in the national organizations and committees which advocate the progress of advanced materials in Egypt. He is a member of the committee of promoting research professors and associate research professors in Mubarak City for Scientific Research and Technology applications. He is also a member in the National Committee of New Materials in the Egyptian Academy of Science and Technology. Prof. Gouda edited a book about the rare early works of Naguib Mahfous, the Egyptian Nobel prize winner in literature. Reuters published a report in Arabic about that book on March 8-2007.



Fouad H. Mahmoud is an Ass. Professor in Mechanical Engineering Department, Shoubra Faculty of Engineering, Banha University, Egypt.



Sayed A. Abd Allah is a Lecturer in Mechanical Engineering Department, Shoubra Faculty of Engineering, Banha University, Egypt.